J Incl Phenom Macrocycl Chem (2017) 88:209–218
DOI 10.1007/s10847-017-0720-x

ORIGINAL ARTICLE

Interaction of isoniazid drug with the pristine and Ni-doped of (4, 4) armchair GaNNTs: a first principle study

M. Rezaei-Sameti[1] · F. Moradi[1]

Received: 2 February 2017 / Accepted: 13 May 2017 / Published online: 17 May 2017

Abstract In this research, the interaction of isoniazid drug (INH) with the pristine and Ni-doped Gallium nitride nanotubes (GaNNTs) is investigated by using density function theory. The adsorption energy, deformation energy, natural bond orbital (NBO), quantum parameters, molecular electrostatic potential (MEP) and thermodynamic parameters of all adsorption models are calculated from optimized structures. The values of adsorption energy, enthalpy and Gibbs free energy of all adsorption models are negative and all adsorption process are favorable in view of thermodynamic points. It is notable that Ni-doped decrease adsorption strength and it is not suitable for INH adsorption on the GaNNTs surface. The MEP, NBO and maximum amount of electronic charge ΔN results demonstrate that the negative potential are localized around adsorption position and the positive potential are localized around INH molecule. The calculated results indicate that the GaNNTs is a good candidate to making absorber and sensor for detecting INH drug.

Keywords GaNNTs · DFT · Isoniazid interaction · Quantum parameters · MEP · NBO

Electronic supplementary material The online version of this article (doi:10.1007/s10847-017-0720-x) contains supplementary material, which is available to authorized users.

✉ M. Rezaei-Sameti
mrsameti@gmail.com

[1] Department of Applied Chemistry, Faculty of Science, Malayer University, Malayer 65174, Iran

Introduction

In the recent years, after discovery and syntheses various nanotube many attentions are focused to experimental and theoretical investigations on the fabrication of materials with nanotube and nanowire structures and properties of these materials due to their remarkable physical, chemical and mechanical properties and thus the great potential applications in nanodevices and technologies. It is well known that these properties are strongly depend on structural organization and also on the presence of vacancies and impurities [1–7].

Gallium nitride nanotubes (GaNNTs) is one of the important nanotubes which have been synthesized by epitaxial casting techniques in 2003. It has been reported that the GaNNTs is an important material due to their mechanical, optoelectronic properties, high thermal, mechanical stability, high-power electronics, short wavelength detectors applications and the band gap of nanotube independent on their chirality [8–19]. In the recent years the extensive researches have been done on the study of doping and interaction metal atoms with different nanotubes due to achieve their applications in many fields, such as detector and adsorbent of various pollution and impurities materials, gas catalysis, hydrogen storage, sensing and the fabrication of magnetic nanodevices [20–25]. Isoniazid, also known as isonicotinylhydrazide (INH) and antituberculosis drug, which is used an antibiotic for the prevention and treatment of both latent and active tuberculosis. It is effective against mycobacteria, particularly *Mycobacterium tuberculosis*. Isoniazid has no clear antiplasmodial activity but delays malaria mortality in mice and reduces overall parasite load when given in combination with rifampicin [26–31].

In the our previous research we studied the CO, O_2, HCN, F_2 and N_2O adsorption on the surface of BPNTs,

AlNNTs, AlPNTs, BPNTs, and BeONTs respectively [32–37]. In this research we investigate the interaction of INH with the pristine and Ni-doped of GaNNTs. The Ni doping may impose changes in the interactions of the nanotubes with INH molecule. For this purpose, we consider 30 different configurations for adsorbing INH on the surface of nanotube at different positions, after optimizing of all considered models at B3LYP/3–21G level of theory we select 24 suitable models for this study (see Fig. 2). The A and B models are used to display adsorption INH on the Ga51 position of pristine and Ni/Ga51 position of Ni-doped of GaNNTs respectively. The C and D models are used to exhibit adsorption INH on the N51 position of pristine and Ni/N51 position of Ni-doped of GaNNTs respectively. The a, b, c, d, e and f are used to show the interaction positions of INH molecule on the surface of GaNNTs (see Fig. 1).

From optimized structures (see Fig. 2) the adsorption energy, gap energy, thermodynamic parameters, NBO, DOS, MEP plots, HOMO–LUMO orbitals and quantum parameters of all models are calculated and results are analyzed. The results of this study should be useful to carry out potential applications of the pristine and Ni-doped GaNNTs as a possible isoniazid sensor or absorber.

Computational details

The electronic structure calculations of all adsorption models are performed with the program Gaussian vG09 [38] at the density functional theory (DFT) approach with cam-B3LYP/6–31G(d) level of theory. The adsorption energy (E_{ads}) of INH/GaNNTs system for all A-a to D-f models are calculated by Eq. 1 and results are listed in Table 1.

$$\Delta E_{ads} = E_{GaNNTs/INH} - (E_{GaNNTs} + E_{INH}) \quad (1)$$

Here the $E_{GaNNTs–INH}$, E_{INH} and E_{GaNNTs} are the potential energy of the GaNNTs/INH complex, GaNNTs and INH respectively.

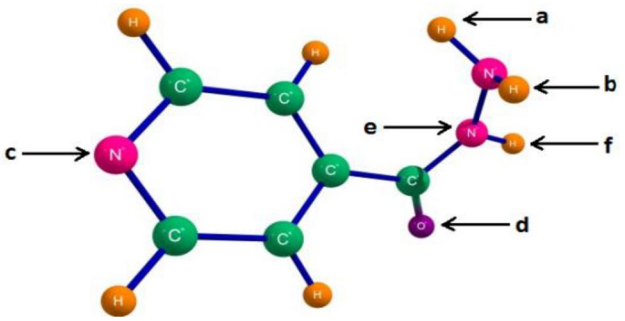

Fig. 1 The optimized structure of isoniazid molecule, *a, b, c, d, e* and *f* are adsorption position

The adsorption energy of nanotube/INH complex can be calculated from interaction energy (E_{int}) and deformation energy (E_{def}) contributions, which are both occurred during the adsorption process. Hence, the following equations are applied to calculate these contributions [39]:

$$E_{\text{int}} = E_{GaNNts-INH} - (E_{GaNNTs\,in\,complex} + E_{INH\,in\,complex}) \quad (2)$$

$$E_{def-GaNNTs} = E_{GaNNTs\,pure} - E_{GaNNTs\,in\,complex} \quad (3)$$

$$E_{def-INH} = E_{INH\,pure} - E_{INH\,in\,complex} \quad (4)$$

$$E_{ads} = E_{total\,def} + E_{\text{int}} \quad (5)$$

where $E_{GaNNTs\ in\ complex}$ is the total energy of GaNNTs in the GaNNTs/INH complex when INH is absent oneself, and $E_{INH\ in\ complex}$ is the total energy of INH molecule in the GaNNTs/INH complex when GaNNTs is absent oneself. The $E_{def\ GaNNTs}$ and $E_{def\ INH}$ are the deformation energy of GaNNTs and INH in its optimized geometry.

The quantum molecular descriptors: the ionization potential (I), the electron affinity (A), energy gap (E_{gap}), electronic chemical potential (μ), global hardness (η), electrophilicity index (ω), global softness (S), electronegativity (χ), Fermi level (E_{FL}), work function ($\Delta\varphi$) and maximum amount of electronic charge ΔN [32–37] of the nanotubes/INH complex are calculated by Eqs. (6–15) from HOMO and LUMO energy:

$$I = -E_{HOMO},\ A = -E_{LUMO} \quad (6)$$

$$E_{gap} = E_{LUMO} - E_{HOMO} \quad (7)$$

$$\mu = -(I + A)/2 \quad (8)$$

$$\eta = (I - A)/2 \quad (9)$$

$$\chi = -\mu \quad (10)$$

$$\omega = \mu^2/2\eta \quad (11)$$

$$S = 1/2\eta \quad (12)$$

$$E_{FL} = 1/2(E_{HOMO} + E_{LUMO}) \quad (13)$$

$$\Delta N = -\mu/\eta \quad (14)$$

$$\Delta\Phi = E_{HOMO} - E_{FL} \quad (15)$$

Results and discussion

Optimized structures and electronic properties

The geometrical and structural properties of isoniazid adsorption on the a, b, c, d, e and f position on the surface of Ga41, Ga41/Ni, N41 and N41/Ni GaNNTs for all stable configurations A-a to D-f models are presented

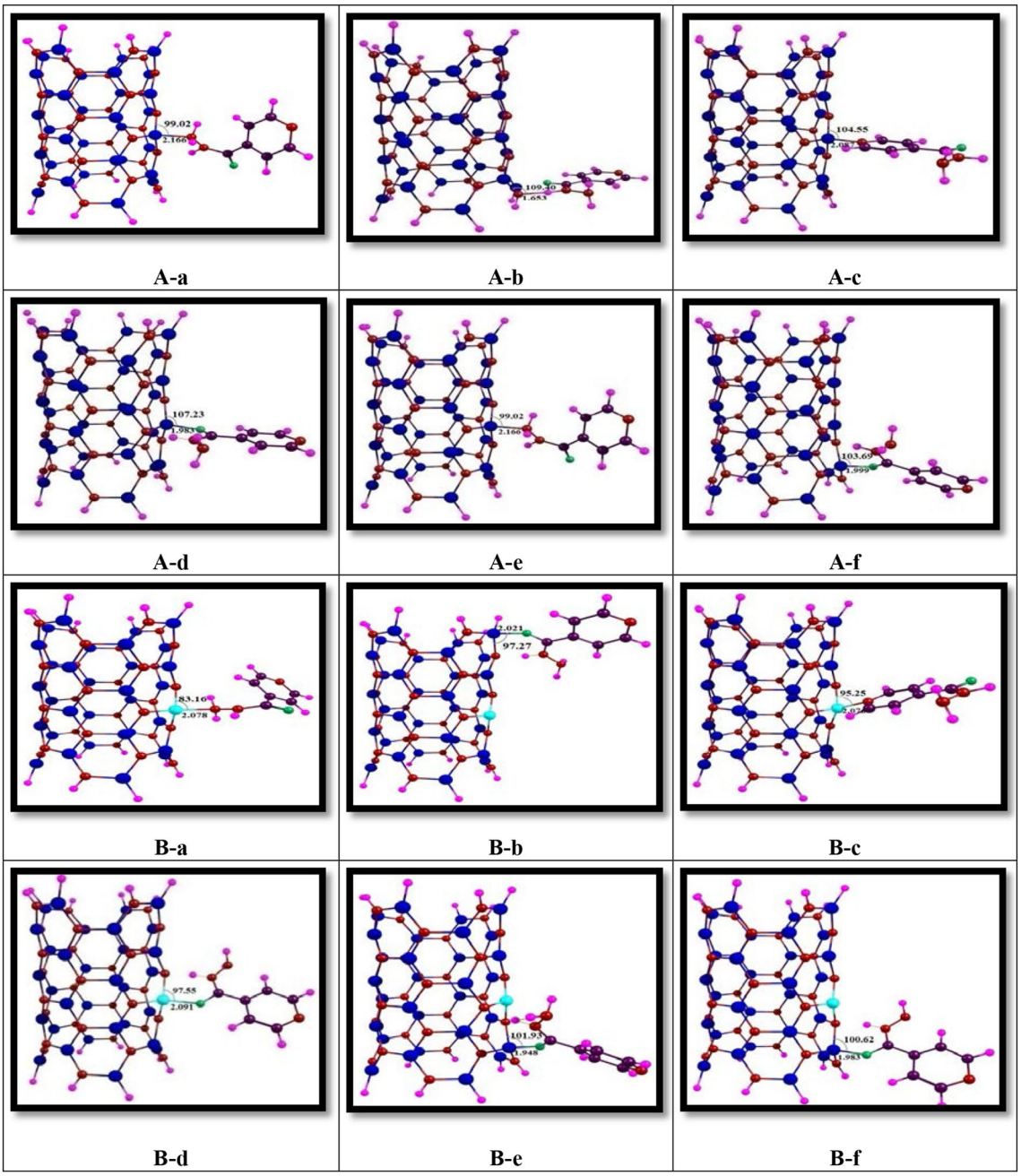

Fig. 2 2D views of adsorption INH drug on the surface of pristine and Ni-doped of (4, 4) armchair GaNNTs for **A-a** to **D-f** optimized models

in Fig. 2. The optimized geometry results show that the title molecule belongs to C1 point group symmetry. The length of optimized pristine (4, 4) armchair GaNNTs nanotube is 11.95 Å and diameters of optimized nanotube 6.95 Å. The calculated binding distance of INH on surface of nanotube are shown in Fig. 2 and, their selected (Ga–N) bond length and (Ga–N–Ga) bond angle around adsorption position of nanotube are given in Tables S1 and S2 in supplementary data. The (Ga–N) bond lengths in pristine GaNNTs are 1.84 Å and in Ni doped is 1.95 Å, this result is in agreement with other researches [18–20]. The calculated results reveal that with adsorbing the INH molecule on the surface of the nanotube, three Ga–N bond lengths and N–Ga–N bond angle of the around of the adsorbing position slightly alter compare to the original values, and this result demonstrate that the bonds length around the site of interaction are weaken. The structural properties consisting of dipole moments (μ_d), the adsorption (E_{ads}), interaction (E_{int}) and deformation (E_{def}) energies of nanotube and INH molecule

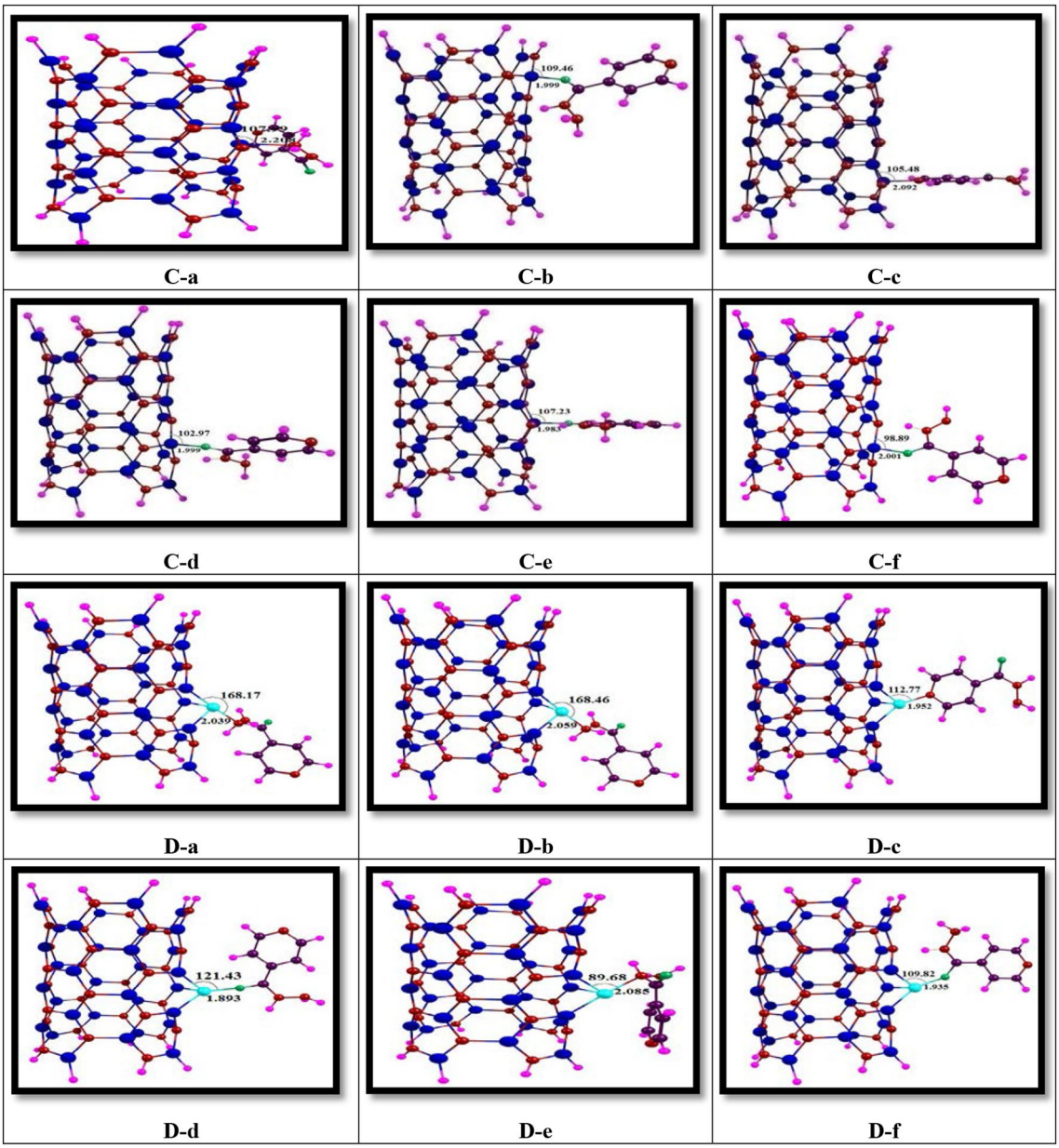

Fig. 2 (continued)

and binding distance for the A, B, C, and D models are summarized in Table 1. The binding distant and bond angle between INH and nanotube is in range 1.68–2.16 Å and 95–168° respectively, these results confirm that the binding INH on nanotube is physisorption. As is evident from Fig. 2 by substituting the N atom with the Ni atom, the geometric structure of the GaNNTs is dramatically distorted. In the optimized Ni-doped in D models, the Ni atom is projected out of the nanotubes surface to reduce stress due to theirs larger size compared to the N atom. On the other hand, the significant changes of geometries are just for those atoms located in the nearest neighborhood of the Ni-doped of GaNNTs whereas those of other atoms remain almost unchanged.

After the optimization process, it is found that the adsorption energy values at all models are negative and all process are exothermic in thermodynamic approach. It is worth mentioning that all systems considered here correspond to energy minima since no imaginary frequencies are observed. The obtained results indicate that the most stable structures are A-d and D-e models with the adsorption energy −107.14 kcal/mol (see Table 1). It is found that the calculated adsorption energy of this complex is strongly depending on adsorption orientation of

Table 1 Calculated adsorption, deformation energy of nanotube, isoniazid and total, binding energy (kcal mol^{-1}) and dipole moment for nanotube and isoniazid at A-a to D-f adsorption models (see Fig. 1)

Property	A-a	A-b	A-c	A-d	A-e	A-f	B-a	B-b	B-c	B-d	B-e	B-f
E_{ads}	−92.23	−103.54	−100.26	−107.14	−97.23	−96.36	−20.07	−34.08	−26.13	−18.97	−29.30	−40.01
$E_{def-GaN}$	72.32	62.51	70.04	65.52	72.31	66.02	−4.50	−3.64	−5.80	−12.01	−12.04	−3.54
$E_{def-INH}$	−3.12	−5.42	−0.64	−4.98	−3.12	−2.73	−2.68	−3.93	−0.60	−5.07	−5.68	−3.98
$E_{def-total}$	−64.19	−57.11	−65.83	−60.81	−69.19	−63.29	7.98	7.55	6.40	17.08	17.73	6.07
E_{int}	−28.00	−46.43	−34.43	−46.59	−28.04	−33.07	−42.00	−41.63	−32.53	−48.01	−47.03	−30.25
μ_d	1.83	4.71	10.13	4.64	1.83	5.25	2.46	4.20	8.62	2.82	2.64	4.20
$D_{bin-distance}$	2.16	1.65	2.08	1.98	2.16	2.00	2.08	2.02	2.07	2.09	1.95	1.98
Property	C-a	C-b	C-c	C-d	C-e	C-f	D-a	D-b	D-c	D-d	D-e	D-f
E_{ads}	−27.80	−26.10	−33.53	−26.79	−21.35	−37.07	−89.80	−100.78	−103.69	−104.84	−107.14	−105.84
$E_{def-GaN}$	−4.39	−9.54	−4.80	−4.00	−8.03	−8.02	72.46	66.02	69.63	66.23	65.53	66.88
$E_{def-INH}$	−2.55	−3.03	−0.88	−1.39	−13.58	−6.70	−6.99	−2.74	−0.63	−3.84	−4.97	−3.95
$E_{def-total}$	7.36	8.90	5.67	4.4	14.26	14.72	−65.47	−62.79	−69.01	−62.39	−60.55	−62.94
E_{int}	−35.16	−35.00	−39.20	−32.19	−35.61	−51.79	−24.33	−37.99	−34.68	−42.48	−46.59	−42.90
μ_d	3.63	5.23	10.38	5.55	4.64	4.74	2.63	2.42	8.44	7.92	3.58	4.46
$D_{bin-distance}$	2.20	2.00	2.09	2.00	1.98	2.00	2.04	2.06	1.95	1.89	2.08	1.94

INH and Ni doped. In the B model, when the Ni atom doped on the Ga41 atoms the adsorption energy at all (a–f) orientation models decrease significantly from pristine models. Whereas, with doping Ni atom on the N41 position the adsorption energy increase significantly from pristine models. It is notable that for pristine models the INH adsorption on the Ga41 position is more favorable than N41 position. Due to values of adsorption energy, we find that the adsorption of INH on the Ga41 in A models and the Ni atom in D models is physical adsorption and polar covalent bonds type. On the other hand, the INH adsorption on the N41 atom in C models and Ni atom in B models is a weak physical adsorption due to weak van der Waals interaction. The adsorption interaction induces little local structural changes on both the INH molecule and the GaN nanotube. The adsorption strengths of INH at the (a) orientation of A, B, C, and D models are in the following order: A-a > D-a > C-a > B-a. Comparison results of Table 1 indicate that the B-d model shows the lowest suitability for INH adsorptions in view of thermodynamic approach. The influence of INH from O-head towards Ga41 site of nanotube (A-d model) and from N2-head towards Ni site of nanotube (D-e model) is more reactive than other those sites of nanotube and INH molecule. To further understanding the effect of INH adsorption on the structural properties of nanotube/INH, the deformation interaction energy of nanotube, INH molecule and nanotube/INH complex are calculated from Eqs. 2–4 and the calculated results are given in Table 1. Inspections of results indicate that the interaction energy of all adsorption models is exothermic. Consequently, a negative value of the interaction energy indicates an attractive interaction between the INH molecule and nanotube; therefore, the combining energy of the hybrid systems is negative. It is notable that the strongest and lowest interaction are occurred in the C-f model and A-a model with −51.79 kcal/mol and −28 kcal/mol respectively. Furthermore, the deformation energy values for the relaxed structures of all adsorption models indicate that significant curvature in the geometry of nanotube and INH molecule is occurred, when the INH molecule adsorbed on the surface of GaNNTs. Comparison results reveal that the deformation energy of nanotube for the A and D models are positive and for the B and C models are negative. The negative value of deformation energy displays that the deformation process of molecule is spontaneous and stable. However, the deformation energies of all models for INH molecule are negative. Furthermore, the deformation energy of INH molecule at the C-e model is more than other those models and B-c model is lower than those model. Comparison results indicate that the more total deformation energy of nanotube/INH complex is occurred in the A and D models. It is known that as the interaction becomes stronger, the deformation degree of the nanotube after absorbing the INH molecule becomes more. It is noticeable that the differences between the dipole moments in these systems can be attributed to nature of impurity atoms. As we can see in Table 1 dipole moment of the A-c, B-c, C-c and D-c models are more than other those models, and are in the following order: C-c > A-c > B-c > D-c; and the high dipole moment illustrates the high reactivity of the title complex (see Fig. 3).

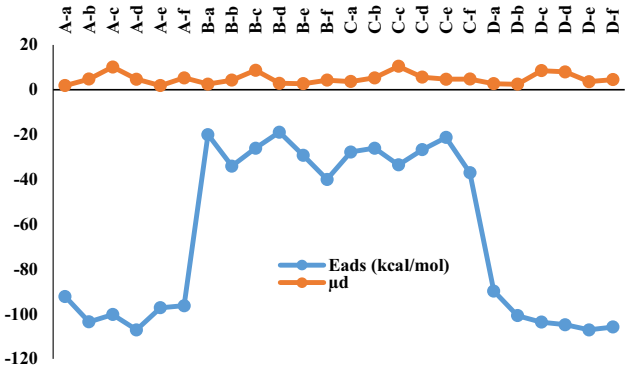

Fig. 3 Comparison of the adsorption energy and dipole moment *A-a* to *D-f* optimized models (see Fig. 1)

Thermodynamic parameters

For deep understanding the interaction of INH molecule and GaNNTs, the thermodynamic parameters such as Gibbs free energy, enthalpy, entropy of system are calculated and results are given in Table 2. As shown in Table 2, the ΔH_{ads} values for all models are negative between −19.86 and −104.21 kcal/mol, showing that the adsorption process is exothermic and favorable in thermodynamic approach. However, the ΔS_{ads} values for all adsorption models are negative and it is unfavorable in thermodynamic approach, because in adsorption process two reactants are combined and produced one product. On the other hand, ΔG_{ads} values of all adsorption models are negative between −5.61 and −89.93 kcal/mol. The negative values of ΔG_{ads} denoted that the adsorption of INH on the surface of pristine and Ni doped GaNNTs is spontaneously in thermodynamic approach. The infrared (IR) spectrum of all adsorption models are calculated and results are given in Fig S1 in supplementary data. Comparison of IR spectrum of all models indicate that the adsorption position are affected on the number of intensity and adsorption peaks.

The natural bond orbital (NBO) analysis

In order to understanding the interaction between INH molecule and nanotube the $\Delta\rho_{(NBO)}$ and $\Delta\rho_{(Mulliken)}$ NBO and Mulliken charge density on the INH molecule is calculated. The ρ_1 and ρ_2 is the NBO or Mulliken charge on the INH molecule before and after adsorbing process respectively. As seen in Table S4 in supplementary data, it is found that the $\Delta\rho_{(Mulliken)}$and $\Delta\rho_{(NBO)}$ values of INH molecule are in range of +0.42 |*e*| to +0.53 |*e*| and +0.44 |*e*| to +0.54 |*e*| respectively. The positive values of the $\Delta\rho_{(Mulliken)}$ and $\Delta\rho_{(NBO)}$ values in all adsorption models confirm that the INH molecule in this process act as

Table 2 Thermodynamic parameters for adsorption isoniazid on GaNNTs for A-a to D-f adsorption models (see Fig. 1)

	ΔE (kcal/mol)	ΔH (kcal/mol)	ΔG (kcal/mol)	ΔS (Cal/mol.K)	ΔCv (Cal/mol.K)
A-a	−92.84	−93.43	−79.78	−45.61	−2.42
A-b	−99.90	−100.49	−86.02	−48.54	−2.68
A-c	−99.31	−98.72	−86.18	−46.03	−2.47
A-d	−103.62	−104.21	−89.93	−47.88	−2.11
A-e	−92.84	−93.43	−79.79	−45.78	−2.42
A-f	−97.10	−97.69	−83.76	−46.70	−1.82
B-a	−19.92	−19.92	−7.30	−42.26	5.44
B-b	−34.93	−34.93	−19.66	−51.21	3.37
B-c	−26.48	−26.48	−11.82	−49.17	3.50
B-d	−19.86	−19.86	−5.61	−47.79	5.64
B-e	−30.56	−30.56	−14.87	−52.61	4.15
B-f	−40.96	−40.96	−25.19	−52.89	3.43
C-a	−85.63	−86.22	−72.68	−44.81	−1.81
C-b	−97.08	−86.22	−72.86	−46.70	−1.82
C-c	−99.17	−99.76	−85.95	−46.33	−2.58
C-d	−101.10	−101.69	−87.30	−48.26	−2.20
C-e	−103.62	−104.21	−89.93	−47.89	−2.11
D-a	−25.63	−26.22	−14.02	−40.93	4.24
D-b	−25.36	−25.95	−11.80	−47.49	5.30
D-c	−32.70	−33.31	−19.49	−46.36	6.16
D-d	−26.25	−26.85	−13.71	−44.06	6.47
D-e	−21.86	−22.45	−7.62	−49.75	6.74
D-f	−36.85	−37.44	−22.86	−48.90	5.53

electron donor. These results confirm that the electron flow spontaneously from the INH molecule toward nanotube. This result is in agreement with the positive values of maximum amount of electronic charge (ΔN) transfer. Comparison results display that the $\Delta\rho_{(NBO)}$ values of B-a and D-a models are more than those other models (see Table S5 in supplementary data).

From NBO results, the interaction between the bond orbitals, antibond orbitals, Rydberg extra valence orbitals, bond bending effect and hybridization and covalency effects in polyatomic wave functions are investigated [40, 41]. For each donor NBO and acceptor NBO, the stabilization energy with delocalization $i \rightarrow j$ is presented as the second-order perturbation interaction energy $E^{(2)}$:

$$E^{(2)} = q_i \frac{F_{ij}^2}{\varepsilon_j - \varepsilon_i} \tag{16}$$

where q_i is donor orbital occupancy ε_i and ε_j are orbital energies and F_{ij} is the off-diagonal NBO Fock matrix element. Delocalization of electron density between occupied and unoccupied orbitals could be considered as acceptor–donor interactions. The extracted results of NBO calculations are given in Table S6 in supplementary data. The selected transition σN42–Ga32 as donor electron orbital and n*G52/Ni orbital as acceptor electron for the A and B models and the selected transition σGa61–N71 as donor electron orbital and RY*N51/Ni orbital as acceptor electron for the C and D models are shown in Fig. 4. As we can see in Fig. 4 the second order perturbation interaction energy $E^{(2)}$ of the A-b, B-f (spin β), C-f and D-a (spin β) is more than other those models. Inspections of NBO results in Table S6 in supplementary data indicate that the most important common interaction with the highest energy $E^{(2)}$ in all models is: in A models transition donor to acceptor orbital a, b, c, d, e and f with $E^2_{/(kcal/mol)} = 46.43$, 7.42, 25.66, 22.97, 46.42, and 4.01 respectively; in B models transition donor to acceptor orbital g, h, i, j, and k with $E^2_{/(kcal/mol)} = 78.37$, 13.45, 10.08, 18.44, 50.23 and 37.64 respectively, in C models transition donor to acceptor orbital m, n, o, p and q with $E^2_{/(kcal/mol)} = 10.20$, 5.38, 6.37, 8.44, 5.36 and 6.99 respectively, in D models transition donor to acceptor orbital r, s, t, x, y and z with $E^2_{/(kcal/mol)} = 126.05$, 127.89, 23.51, 14.94, 34.29 and 27.73 respectively(see Table S6 in supplementary data).

These results display that the transition from donor orbital to acceptor orbital depend to position of adsorbent and doping atom. It is notable that the doping impurity atoms in nanotube change significantly the $E^{(2)}$ values and charge transfer between donor and acceptor orbitals. These results lead to Ni-doped GaNNTs having higher polarizability than INH molecule, and so the INH adsorption change significantly the electrical properties of nanotube from original state.

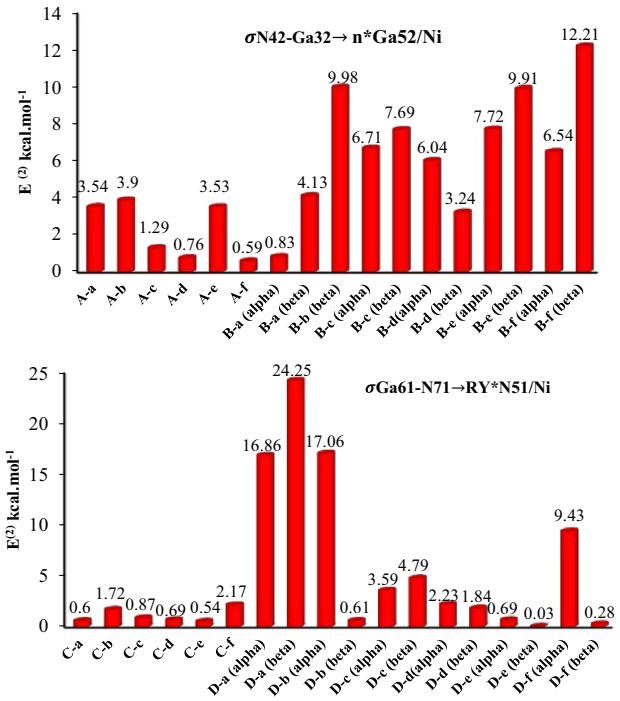

Fig. 4 The stabilization energy ($E^{(2)}$) of donor and acceptor orbitals for adsorption isoniazid on GaNNTs for *A-a* to *D-f* optimized models (see Fig. 1)

The interactions of some molecular orbitals of the two constituents in the favorable adsorption systems with the largest $E^{(2)}$ values show the more intensive interaction between donor and electron acceptor bonding or antibonding orbitals considered. The results of NBO analysis confirm that intermolecular interaction of this complex is stronger than the other complexes because of more total charge transfer energy. In addition, it is found that the greatest stabilization energy for Ni-doped complex is accordance with the shortest interaction distance.

QTAIM calculations

For deep understanding the electrical properties of INH adsorption on the surface of GaNNTs, the electron's wave functions are extracted from the optimized structures, and according to Bader's quantum theory of atoms in molecules (QTAIM), electron densities (ρ) and Laplacian of electron, densities ($\nabla^2\rho$) at bond critical point (BCP) were calculated using AIMALL program [42–44]. The properties ρ_{BCP}, $\nabla^2\rho$, the total electronic energy (H_{BCP}), the potential energy (V_{BCP}) and the kinetic energy (G_{BCP}) of the bond critical points are closely related to the type and strength of the interactions between the attractive atom pairs. The properties of ρ_{BCP}, $\nabla^2\rho$, H_{BCP}, V_{BCP}, and G_{BCP} for the A-a,

A-b, A-c, A-d, A-e, B-b, B-e, C-a, C-b, C-d, C-f, D-c and D-f due to binding INH and GaNNTs are calculated and all results are listed in Table S7 in supplementary data. The value of ρ_{BCP} can reflect the interaction strength. The ρ_{BCP} of the D-f (0.3229) and B-e model (0.04481) is significantly larger than those other adsorption models. In addition, the D-f model possesses the more positive H_{BCPs} and the larger absolute values of $\nabla^2\rho$, G_{BCP}, and V_{BCP} than other those models. These results indicate that the covalent bonding interactions between INH and nanotube are stronger than those other models. So should be more effective to adsorb and sense INH. The values of G_{BCP} and V_{BCP} for all adsorption models are positive. Comparison results show that in the A-a, A-b, A-c, A-e, C-b, C-d, D-c and D-f models the $\nabla^2\rho$ and H_{BCP} are positive. The positive values of all $\nabla^2\rho$ confirm the noncovalent nature of these interactions. With respect to the sign of Laplacian of electron density on BCPs data, existence of electrostatic type of interactions, which is a subset of noncovalent interactions, would be proved.

Molecular electrostatic potential

For determining the molecular size, shape as well as positive, negative and neutral electrostatic potential regions in terms of color grading the molecular electrostatic potential (ESP) are calculated for all adsorption models [45–47]. The electrostatic potential (ESP) and contour potential of all adsorption models are given in Fig. S2 in supplementary data. In case of ESP, the red color represents the negative charges or the electrophilic regions and the blue color represents the positive charges or the nucleophilic regions. According to the result of Fig. S2 in supplementary data, there is a significant electron density, and negative potential, red, around nanotube adsorption position and the positive potential, blue color, are localized around INH molecule. It indicates that a low charge is transferred from the INH molecule toward the nanotube ones resulting in a weak ionic bonding in the GaNNTs/INH complex. Therefore, it is expected that the interaction between INH molecule and nanotube, after adsorption process, caused that the exterior layer of nanotube rich of charge and INH molecule surface poor of charge. The contour map of all models show that the layers of red color strongly overlap on around adsorbent compound and the blue color layers strongly overlap on far from adsorption position.

HOMO and LUMO orbitals

The HOMO (the highest occupied molecular orbital) and the LUMO (the lowest unoccupied molecular orbital) orbital energy are used to understand the nature and electrical properties of GaNNTs/INH complex. Based on the 72 HOMO and LUMO configuration models of INH molecule in Fig. S3 in supplementary data, it can be observed that for pristine model of GaNNTs in the A and C models the HOMO orbital density are almost uniformly distributed through the Ga–N bond of nanotube, due to donor electron effect of INH on the surface of nanotube. On the other hand in the B and D models, the HOMO orbital density is localized on the around Ni doped position of nanotube. It is notable that the LUMO orbital density is localized around INH molecule. In all models after INH adsorption the nucleophilicity of nanotube electrophilicity of INH molecule are increased. The positive values of $\Delta\rho$ of NBO and Mulliken confirm this process. The energy gaps (E_g) between HOMO and LUMO for all adsorption models are calculated and results are listed in Table S8 in supplementary data. As we can see in Table S8 in supplementary, with doping Ni atom the spin of electrons split to α and β spin (see models B and D) on the other hand, the E_g values of all adsorption models are in range 3.61–6.49 eV. It is notable that with doping Ni atom, the E_g values for spin α of B and D models decrease significantly from original values and so the conductivity of system increases. Whereas with adsorbing INH the E_g values for different configuration of INH adsorption alter slightly from original states. From HOMO and LUMO results the density of state (DOS) plots of all adsorption models are calculated in range −15 to +10 eV by using GaussSum software and results are shown in Fig. S4 in supplementary data. In the HOMO and LUMO region, 8 and 13 peaks are displayed respectively. It is clearly observed that in virtual orbitals more peak maxima are observed than occupied orbital. The altitude of all peaks in the HOMO and LUMO region change slightly from original values and with doping Ni atom in the gap region it can be seen one and two small peaks and then due to this peak the Eg values of this system decrease and conductivity of complex increase. These results confirm that Ni doped is a good candidate to increase the conductivity of GaNNTs and to making the sensor for detecting INH molecule. The electronic chemical potential (μ), global hardness (η), electrophilicity index (ω), electronegativity (χ), Fermi level (E_{FL}), and maximum amount of electronic charge ΔN of the nanotubes/INH complex are calculated by Eqs. (6–14) and results are listed in Table S8 in supplementary data.

Inspections of results show that the global hardness (η) values of all adsorption models are in range 1.8–3.97 eV. Comparison results reveal the between global hardness and the adsorption energy there is a linear relation, with increasing global hardness the adsorption energy increase.

The electronegativity (χ) values are in range 3.32–5.15 eV; the electronic chemical potential (μ) are in range −3.23 to −5.15 eV, and the maximum amount of electronic charge ΔN are in range 1.31–2.41. The positive

values of ΔN confirm that in all models, the INH molecule has a donor electron effect and this result is in agreement with NBO and HOMO–LUMO results. Comparison results of the pristine and Ni-doped GaNNTs with all adsorption models reveal that the electronic chemical potential (μ) values of all adsorption models slightly more that original values and so adsorbing INH molecule increase the μ and decrease the stability of system. Table S8 in supplementary data also shows that the Fermi level (E_{FL}) of the GaNNTs increase slightly upon the adsorption of INH molecule. The Fermi level is at the center of the Eg and equal to the chemical potential. Clearly, the change of E_{FL} of nanotubes in adsorption process modified its field emission currents. It is found that HOMO energy of nanotube is increased after adsorption of INH molecules on the surface of nanotube. These results reveal that the interaction of INH molecule with nanotube reduce their nucleophilic reactivates. To study the field emission properties of INH molecule with nanotube the work function ($\Delta\Phi$) of system is calculated by Eq. 15. However, Eq. 17 theoretically describes the emitted electron current densities in a vacuum

$$J = AT^2 \exp^{(-\Delta\Phi/KT)} \quad (17)$$

Here A and T are the Richardson constant (A/m^2) and temperature (K) respectively. The calculated results reveal that the work function of the all adsorption models is in range of −1.81 to −3.25 eV. A negative work function change the donation of charge occurred from the INH molecule toward the nanotube surface. Comparison results show that the emitted electron current density of A-a, A-e and C-a models are more than other those models.

Conclusions

In this theoretical research, we focused on the investigation of interaction between INH drug with pristine and Ni-doped GaNNTs for employing them in possible sensor and adsorption application. Inspections of results indicate that the interaction energy of all adsorption models is exothermic. It is notable that the strongest and lowest interaction are occurred in the C-f model and A-a model with −51.79 kcal/mol and −28 kcal/mol respectively. The obtained results indicate that the most stable structures are A-d and D-e models with the adsorption energy −107.14 kcal/mol. It is found that the $\Delta\rho_{(Mulliken)}$ and $\Delta\rho_{(NBO)}$ values of INH molecule are in range of +0.42 |e| to +0.53 |e| and +0.44 |e| to +0.54 |e| respectively. The positive values of the $\Delta\rho_{(Mulliken)}$ and $\Delta\rho_{(NBO)}$ values in all adsorption models confirm that the INH molecule in this process act as electron donor. These results confirm that the electron spontaneously flow from the INH molecule toward nanotube. A negative work function change the donation of charge occur from the INH molecule toward the nanotube surface. Comparison results show that the emitted electron current density of A-a, A-e and C-a models are more than other those models.

Acknowledgements Authors thank from the nano computational centre of Malayer Universities for supporting this project.

References

1. Dresselhaus, M.S., Dresselhaus, G., Avouris, P.: Carbon nanotubes, synthesis, structure, properties and applications. Springer, Berlin (2001)
2. Ferreira, M.D., Santos, J.D., Taft, C.A., Longo, E., Martins, J.B.L.: Single walled MgF_2 nanotubes. Comput. Mater. Sci. **46**, 233–238 (2009)
3. Sodre, J.M., Longo, E., Taft, C.A., Martins, J.B.L., Santos, J.D.: Electronic structure of GaN nanotubes. C. R. Chim. **20**, 190–196 (2017)
4. Drygas, M., Czosnek, C., Paine, R.T., Janik, J.F.: Aerosol-assisted vapor phase synthesis of powder composites in the target system GaN/TiN for potential electronic applications. Mater. Res. Bull. **40**, 1136–1142 (2005)
5. Zhang, J., Meguid, S.A.: On the piezoelectric potential of gallium nitride nanotubes. Nano Energy **12**, 322–330 (2015)
6. Wu, G., Chen, Y.S., Xu, B.Q.: Remarkable support effect of SWNTs in Pt catalyst for methanol electrooxidation. Electrochem. Commun. **7**, 1237–1243 (2005)
7. Lan, Y., Lin, F., Li, Y., Dias, Y., Wang, H., Liu, Y., Yang, Z., Zhou, H., Lu, Y., Bao, J., Ren, Z., Crimp, M.A.: Gallium nitride porous microtubules self-assembled from wurtzite nanorods. J. Cryst. Growth **415**, 139–145 (2015)
8. Goldberger, J., He, R., Zhang, Y., Lee, S., Yan, H., Choi, H. J., Yang, P.: Single-crystal gallium nitride nanotubes. Nature **422**, 599–602 (2003)
9. Rouhi, S.: Molecular dynamics simulation of the adsorption of polymer chains on CNTs, BNNTs and GaNNTs. Fibers. Polym. **17**, 333–342 (2016)
10. Liliental-Weber, Z., Chen, Y., Ruvimov, S., Washburn, J.: Formation mechanism of nanotubes in GaN. Phys. Rev. Lett. **79**, 2835–2838 (1997)
11. Valedbagi, S., Mohammad Elahi, S., Abolhassani, M.R., Fathalian, A., Esfandiar, A.: Effects of vacancies on electronic and optical properties of GaN nanosheet: a density functional study. Opt. Mater. **47**, 44–50 (2015)
12. Park, Y.S., Lee, G., Holmes, M.J., Chan, C.C.S., Reid, B.P.L., Alexander Webber, J.A., Nicholas, R.J., Taylor, R.A., Kim, K.S., Han, S.W., Yang, W., Jo, Y., Kim, J.: Surface-effect-induced optical bandgap shrinkage in GaN nanotubes. Nano Lett. **15**(7), 4472–4476 (2015)
13. Lee, S.M., Lee, Y.H., Hwang, Y.G., Elsner, J., Porezag, D., Frauenheim T.: Stability and electronic structure of GaN nanotubes from density-functional calculations. Phys. Rev. B **60**, 7788–7795 (1999)
14. Zhang, M., Su, Z.M., Yan, L.K., Qiu, Y.Q., Chen, G.H., Wang, R.S.: Theoretical interpretation of different nanotube morphologies among Group III (B, Al, Ga) nitrides. Chem. Phys. Lett. 408, 145–149 (2005)
15. Behzad, S.: Electronic structure, optical absorption and energy loss spectra of GaN graphitic sheet. J. Mater. Sci. Mater. Electron. **26**, 9898–9906 (2015)
16. Dai, X., Messanvi, A., Zhang, H., Durand, C., Eymery, J., Bougerol, C., Julien, F.H., Tchernycheva, M.: Flexible light-emitting

diodes based on vertical nitride nanowires. Nano Lett. **15**, 6958–6964 (2015)
17. Gobler, C., Bierbrauer, C., Moser, R., Kunzer, M., Holc, K., Pletschen, W., Keohler, K., Wagner, J., Schwaerzle, M., Ruther, P., Paul, O., Neef, J., Keppeler, D., Hoch, G., Moser, T., Schwarz, U.T..: GaN-based micro-LED arrays on flexible substrates for optical cochlear implants. J. Phys. D **47**, 205401–205410 (2014)
18. Hemmingsson, C., Pozina, G., Khromov, S., Monemar, B.: Growth of GaN nanotubes by halide vapor phase epitaxy. Nanotechnology **22**, 085602–085620 (2011)
19. Ismail-Beigi, S.: Electronic excitations in single-walled GaN nanotubes from first principles: dark excitons and unconventional diameter dependences. Phys. Rev. B **77**, 035306 (2008)
20. Star, A., Joshi, V., Skarupo, S., Thomas, D., Jean-Christophe, P.G.: Gas sensor array based on metal-decorated carbon nanotubes. J. Phys. Chem. B **110**, 21014–21020 (2006)
21. Han, W., Bando, Y., Kurashima, K., Sato, T.: Boron-doped carbon nanotubes prepared through a substitution reaction. Chem. Phys. Lett. **299**, 368–373 (1999)
22. Ricardo, A., Guirado-Lopez, M.S., Rincon, M.E.: Interaction of acetone molecules with carbon-nanotube-supported TiO2 nanoparticles: possible applications as room temperature molecular sensitive coatings. J. Phys. Chem. C **111**, 57–65 (2007)
23. Dag, S., Ozturk, Y., Ciraci, S., Yildirim, T.: Adsorption and dissociation of hydrogen molecules on bare and functionalized carbon nanotubes. Phys. Rev. B **72**, 155404–155410 (2005)
24. Lu, Y.J., Li, J., Han, J., Ng, H.T., Binder, C., Partridge, C., Meyyappan, M.: Room temperature methane detection using palladium loaded single-walled carbon nanotube sensors. Chem. Phys. Lett. **391**, 344–348 (2004)
25. Mukhopadhyay, I., Hoshino, N., Kawasaki, S., Okino, F., Hsu, W.K., Touhara, H.: Electrochemical Li insertion in B-doped multiwall carbon nanotubes. J. Electrochem. Soc. **49**, A39–A44 (2002)
26. Eatontown, N.J.: Isoniazid. West-Ward Pharmaceutical Corp., Eatontown (2014)
27. Atlanta, G.A.: Isoniazid. Mikart, Inc., Atlanta (2015)
28. Princeton, N.J.: Isoniazid. Sandoz, Inc., Holzkirchen (2009)
29. Wei, C.J., Lei, B., Musser, J.M., Tu, S.C.: Isoniazid activation defects in recombinant Mycobacterium tuberculosis catalase-peroxidase (KatG) mutants evident in InhA inhibitor production. Antimicrob. Agents Chemother. **47**, 670–675 (2003)
30. Alger, N.E., Spira, D.T., Silverman, P.H.: Inhibition of rodent malaria in mice by rifampicin. Nature **227**, 381–382 (1970)
31. Nayak, P., Swati Patankar, A., Madhusudhan, B.: Assessment of in vivo antimalarial activity of rifampicin, isoniazid, and ethambutol combination therapy. Parasitol. Res. **106**, 1481–1484 (2010)
32. Rezaei-Sameti, M., Yaghoobi S.: Theoretical study of adsorption of CO gas on pristine and AsGa-doped (4, 4) armchair models of BPNTs. Comput. Conds. Matter **3**, 21–29 (2015)
33. Rezaei-Sameti, M., Kazemi, A.: A computational study on the interaction between O_2 and pristine and Ge-doped aluminum phosphide nanotubes. Turk. J. Phys. **39**, 128–136 (2015)
34. Rezaei-Sameti, M., Saki, F.: The interaction of HCN gas on the surface of pristine, Ga, N and GaN-doped (4, 4) armchair models of BPNTs: a computational approach. Phys. Chem. Res. **3**(4), 265–277 (2015)
35. Rezaei-Sameti, M., Dadfar, E.A.: The effects of F_2 adsorption on NMR parameters of undoped and 3Cdoped (8, 0) zigzag BPNTs. Iran. Chem. Commun. **4**, 1–12 (2016)
36. Rezaei-Sameti, M., Samadi Jamil, E.: The adsorption of CO molecule on pristine, As, B, BAs doped (4, 4) armchair AlNNTs: a computational study. J. Nanostruct. Chem. **6**,197–05 (2016)
37. Rezaei-Sameti, M., Hemmati, N.: N_2O interaction with the pristine and 1Ca- and 2Ca-doped beryllium oxide nanotube: a computational study. J. Nanostruct. Chem. **6**, 343–355 (2016)
38. Frisch, M.J., et al.: Gaussian 09, Revision A.02, Gaussian Inc. Wallingford (2009)
39. James, C., Amalraj, A., Reghunathan, R., Hubert Joe, I., Jaya Kumar, V.S.: Structural conformation and vibrational spectroscopic studies of 2, 6-*bis* (p-*N, N*-dimethyl benzylidene) cyclohexanone using density functional theory. J. Raman. Spectrosc. **37**, 1381–1392 (2006)
40. Na, L.J., Rang, C.Z., Fang, Y.S.: Study on the prediction of visible absorption maxima of azobenzene compounds. J. Zhejiang Univ. Sci. **6**, 584–589 (2005)
41. Keresztury, G., Holly, S., Varga, J., Besenyei, G., Wang, A.V., Durig, J.R.: Vibrational spectra of monothiocarbamates-II. IR and Raman spectra, vibrational assignment, conformational analysis and ab initio calculations of *S*-methyl-*N, N*. Spectrochim. Acta Part A **49**, 2007–2017 (1993)
42. Bader, R.F.W.: Atoms in Molecules: A Quantum Theory. Oxford University Press, New York (1990)
43. Biegler-Konig, F.: AIM2000 Designed. University of Applied Sciences, Bielefeld (2001)
44. Shahabi, M., Raissi, H.: Investigation of the molecular structure, electronic properties, AIM, NBO, NMR and NQR parameters for the interaction of Sc, Ga and Mg-doped (6, 0) aluminum nitride. J. Incl. Phenom. Macrocyc. Chem. **84**, 99–114 (2016)
45. Peralta-Inga, Z., Lane, P., Murray, J. S., Boyd, S., Grice, M.E., O'Connor, C.J., Politzer, P.: Characterization of surface electrostatic potentials of some (5, 5) and (n, 1) carbon and boron/nitrogen model nanotubes. Nano. Lett. **3**(1), 21–28 (2003)
46. Bulat, F., Toro-Labbe, A., Brinck, T., Murray, J. S., Politzer, P.: Quantitative analysis of molecular surfaces: areas, volumes, electrostatic potentials and average local ionization energies. J. Mol. Model. **16**(11), 1679–1691 (2010)
47. Bulat, F.A., Burgess, J.S., Matis, B.R., Baldwin, J.W., Macaveiu, L., Murray, J.S., Politzer, P.: Hydrogenation and fluorination of graphene models: analysis via the average local ionization energy. J. Phys. Chem. A **116**(33), 8644–8652 (2012)